第 35 卷 第 3 期
2018 年 9 月

原 子 核 物 理 评 论
Nuclear Physics Review

Vol. 35, No. 3
Sep., 2018

Article ID: 1007-4627(2018) 03-0278-09

Research on Plasma Discharge for Plasma Processing of a 1.3 GHz Single-cell SRF Cavity

YANG Lei[1,2], WU Andong[1,2], LU Liang[1,†], LI Yongming[1], XU Xianbo[1], CHEN Long[1,2], LI Chenxing[1], SUN Liepeng[1], LI Chunlong[1], MA Wei[1,2], HE Tao[1,2], XING Chaochao[1,2], HE Yuan[1]

(*1. Institute of Modern Physics, Chinese Academy of Sciences, Lanzhou 730000, China;*
2. University of Chinese Academy of Sciences, Beijing 100049, China)

Abstract: Field emission limits the accelerating gradient increase in SRF cavities. In order to reduce field emission of SRF cavities, the plasma processing experimental setup of a 1.3 GHz single-cell SRF cavity is designed and built to carry out plasma processing discharge research at room temperature. The electromagnetic field distribution is simulated and the external quality factor is optimized to provide a suitable discharge condition using CST software. It is explored that the physical property of Ar/Ar-O_2 discharge and the variation trend of electron excitation temperature with the changes of pressure, forward power and O_2 content in experiment. The result of residual gas analysis indicates that Ar/O_2 plasma processing can eliminate the carbide of the inner surface of cavity.

Key words: Plasma processing; Ar/Ar-O_2 discharge condition; electron excitation temperature; SRF technology

CLC number: O571.6; P142.9 **Document code:** A **DOI:** 10.11804/NuclPhysRev.35.03.278

1 Introduction

High accelerating gradient is one of the main criterions for the performance of superconducting radio-frequency (SRF) particle accelerator. In most cases, field emission limits the increase of accelerating gradient for SRF cavities[1–2]. Electrons are accelerated and leave the inner surface of cavity beyond the electric field threshold. The gained energy of the electrons is deposited on the surface of SRF cavity by collision, resulting in the increase of the local temperature and the risk of thermal breakdown of superconductivity.

Field emission in SRF cavities can be enhanced by hydrocarbon contaminations usually accumulated in a long-term operation[3]. Some studies show that plasma processing (plasma cleaning) is an effective method to remove hydrocarbon contaminants in SRF cavities[4]. With plasma created, the ions bombard and etch the inner surface of SRF cavities. With some chemical and physical reactions, the contaminants are transformed into volatile states, which can be easily pumped away. Plasma processing is safe, environment-friendly, and economical, compared with traditional processing methods of SRF cavities such as EP (Electric Polishing), BCP (Buffered Chemical Polishing), HPR (High pressure rinsing). According to the experience of Institute of Modern Physics (IMP), the period of processing SRF cavities with the traditional methods is relatively long (generally three month). However, plasma processing can be applied *in situ*, so the processing period can be reduced greatly, which is significant for ensuring the availability of the accelerator facility.

In order to acquire the discharge conditions in SRF cavities, studies of discharge with Ar and Ar-O_2 mixture are performed on a 1.3 GHz single-cell SRF cavity. And the characteristics of discharge are observed as well. We will present the results of these studies. Before launching the experiment, the electromagnetic field distribution is studied with CST[5] so as to design the antenna structure and decide the optimal coupling factor. The physical properties of Ar/Ar-O_2 plasma have direct impact on the perfor-

Received date: 5 Jun. 2018; **Revised date:** 22 Jul. 2018

Foundation item: National Natural Science Foundation of China(91426303, 11475232, 11535016)

Biography: YANG Lei(1992–), male, Chongqing, Ph.D, studying in the field of accelerator; E-mail: yanglei@impcas.ac.cn

† **Corresponding author:** LU Liang, E-mail: luliang@impcas.ac.cn.

mance of the SRF cavities after the plasma processing. To study the Ar/Ar-O_2 discharge conditions, we mainly focus on the forward power of breakdown point and the power reflection coefficient with different pressure and oxygen content. The electron excitation temperature is evaluated and the change of the temperature is studied as functions of pressure, forward power and O_2 content by means of optical emission diagnostics.

2 Experimental setup

Fig. 1 shows the schematic diagram of the experimental setup for plasma discharge. As a whole the setup is composed of a gas control system, a power control system, a cavity system, a vacuum system and an optical emission diagnostics system. The gas control system includes three mass flow meters (ALICAT SCIENTIFIC: 21-1-16-0-50-30-0.25VCRM), a gas mixing chamber, vacuum gauge (PFEIFFER VACUUM: PKR 361). The power control system consists of a power generator (BBEF[6]: RF power generator), a signal generator (ROHDE SCHWARZ: Signal generator), directional couplers and a power meter (BOONTON: 4531 RF power meter). The cavity system is made up of a 1.3 GHz single-cell SRF cavity and a variable coupler. The major parameters of the experimental cavity are listed in Table 1. There is a mechanical pump (PFEIFFER VACUUM: ACP 40) and a turbo molecular pump (PFEIFFER VACUUM: HiPace 80) in the vacuum system. The optical emission diagnostics system contains a spectrometer (AVANTES: AvaSpec-2048FT-4-DT) and an optical fiber.

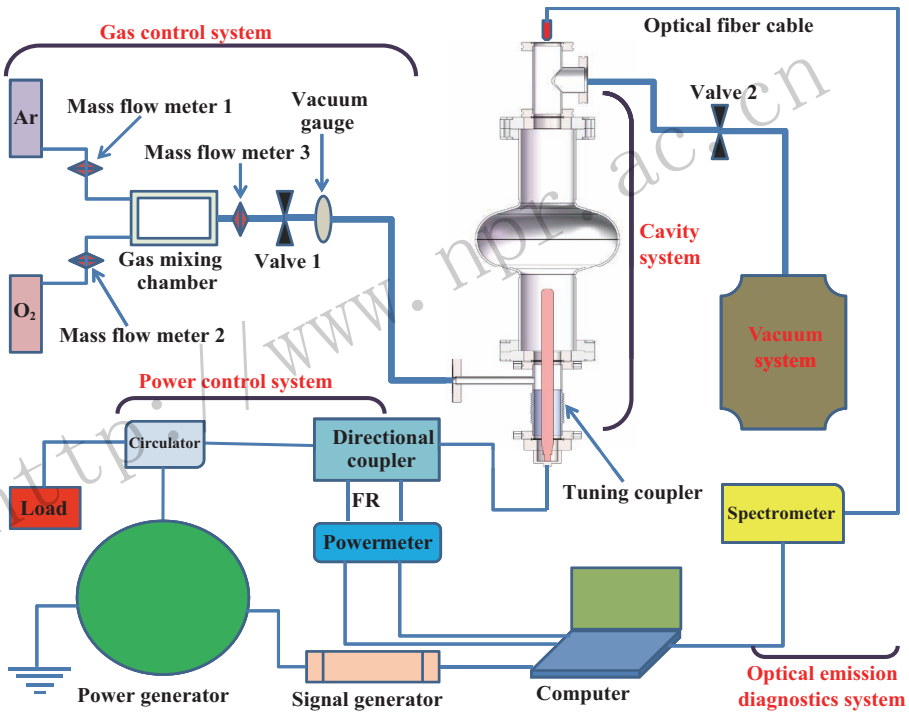

Fig. 1　(color online) Schematic diagram of the setup for Ar/Ar-O_2 plasma discharge experiment.

Table 1　Main Parameters of the 1.3 GHz single-cell SRF cavity at 2 K.

Parameter	Value
Frequency/GHz	1.3
Unload factor (Q_0)	1.5×10^{10}
Ep/E_{acc}	1.84
G/Ω	277.8
R/Q_0	104.6

Fig. 2 exhibits the exact experimental setup. RF power, generated from the solid amplifier, is feed to the cavity with the transmission line and the coupler. On one of the beam pipe flanges, the variable coupler is mounted, on which the gas input port is located. On the other beam pipe flange, there is a three-channel pipe which provides the vacuum port and the view port. On one hand, a vacuum port of three-channel pipe is connected to the pump system (a mechanical pump and a turbo molecular pump). One vacuum gauge is used to measure the gas pressure of the cavity. Three mass flow meters are used to monitor the gas flow of pure Ar, pure O_2 and Ar-O_2 mixture. On the other hand, through the view port, the Ar/Ar-O_2 plasma optical emission spectrum is detected by the spectrometer. In addition, the forward power and reflected power signals are picked up with the directional couplers.

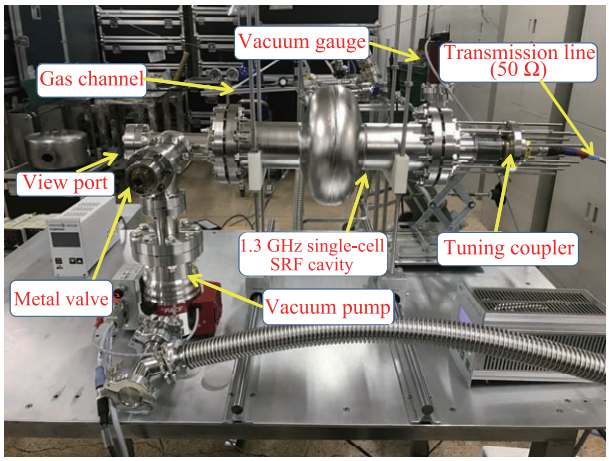

Fig. 2 (color online) The details of the 1.3 GHz single-cell SRF cavity plasma processing experimental setup.

3 Electromagnetic field mode and the external quality factor for ignition

In our case, plasma is believed to be created by the ionization of gas molecules with the presence of intense RF fields, which cause electrical insulation broken down. Such a process eventually brings about plenty of charged particles, electron/ions[7]. Generally, the plasma is only generated in the E-field (electric field) region, rather than in the magnetic region[8]. So E-field distributions affect the distributions of plasma greatly. The ideal discharge for processing is that plasma distributes uniformly on the inner surface of the cavity. In the experiment, the fundamental mode (TM010) is utilized, whose E-field distribution is simulated with CST and is presented in Fig. 3. Judging from Fig. 3, it seems difficult to realize ideal discharge due to the non-uniform E-field distribution. However, we find TM010 mode is the lowest mode that can be used to generated strong electrical field rightly located on iris region. And, the iris region is where field emission happens most frequently, which should be processed with special attention. As a result, the iris region will be particularly processed using TM010 as the ignition RF mode. Although uniformly processing is not achieved, the processing effect is expected to be good.

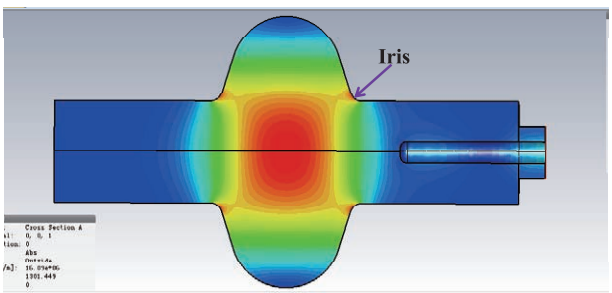

Fig. 3 (color online) The electric field distribution simulated by CST in the experimental cavity.

The RF power is feed to the cavity with the variable coupler. The input power is consumed by the cavity wall and the plasma. Precisely measuring the power loss by plasma has not been achieved by far. The eigen quality factor (Q_0) is approximately 8838, measured by a Vector Network Analyzer in room temperature. To minimize the reflected power, the coupling of about 1 is chosen. Therefore, a suitable external quality factor (Q_e) should be acquired, which is decided by the length of the antenna for the chosen straight antenna (copper or niobium), as shown in Fig. 4. Fig. 5 shows the distribution of the external quality factor with varying antenna length inside the cavity. The length of the antenna inside the cavity is chosen as 90 mm so as to get the desired Q_e.

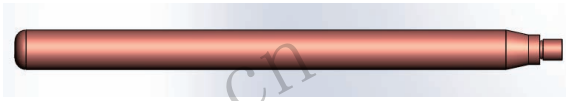

Fig. 4 (color online) A diagram of the coupling straight antenna.

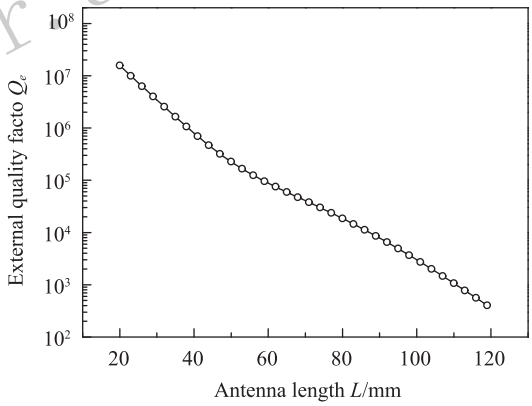

Fig. 5 (color online) The external quality factor changes with the length of the antenna inside the cavity.

4 Method for electron excitation temperature measurement

In plasma discharge, there is an important physical quantities called ion energy ($\xi_{\rm wall}$) in inner surface of cavity. We can get its value from the potential of presheath to boundary ($\phi_{\rm pd}$)[9],

$$\phi_{\rm pd} = -\frac{T_{\rm exc}}{2}\left[\ln\left(\frac{M_{\rm i}}{2\pi m_{\rm e}}\right)+1\right] \tag{1}$$

$T_{\rm exc}$ is electron excitation temperature. $M_{\rm i}$ is the mass of ion, and $m_{\rm e}$ is the mass of electron. With Ar as discharge gas, we can get $\xi_{\rm wall}$=5.2 $T_{\rm exc}$ in inner surface of cavity. Thus, it is necessary for us to measure $T_{\rm exc}$.

We employ the optical emission diagnostics method to obtain the electron excitation temperature. The state of plasma can be determined by measuring

its optical emission spectroscopy, the most reliable no-intruding technique[10]. If the upper levels of the selected atomic transitions reach the LTE (local thermodynamic equilibrium) state, then the conventional Boltzmann plot technique can be employed to acquire the excitation temperature[11]. Ref. [12] has elucidated the fundamental principles of the conventional Boltzmann plot method in detail.

For two energy levels in their thermal equilibrium state, the relation between their energy levels and atomic densities can be express by Boltzmann distribution

$$\frac{N_{\rm k}}{N_{\rm i}}=\frac{g_{\rm k}}{g_{\rm i}}\exp\left|-\frac{E_{\rm k}-E_{\rm i}}{KT_{\rm exc}}\right|, \tag{2}$$

$E_{\rm i}$ and $E_{\rm k}$ are the lower and upper energy level, respectively. $N_{\rm i}$ and $N_{\rm k}$ denote the corresponding atomic densities, $g_{\rm i}$ and $g_{\rm k}$ represent the statistical weights for the corresponding states, and K is Boltzmann constant. Assuming the total population density is N, the Boltzmann relation for a given atomic state can be given by applying equation (2)

$$\frac{N_{\rm k}}{N}=\frac{g_{\rm k}}{Z(T)}\exp\left|-\frac{E_{\rm k}-E_{\rm i}}{KT_{\rm exc}}\right|, \tag{3}$$

Z(T) is partition function given by

$$Z(T)=\sum_m g_m\exp\left|-\frac{E_m}{KT_{\rm exc}}\right|, \tag{4}$$

indicating the sum of the weighted Boltzmann function of all the discrete energy levels. When the plasma atom gets de-exited and comes back to $E_{\rm i}$ from $E_{\rm k}$, then we can obtain the emission coefficient of spectral line (ε_{ki})by using the equation

$$\varepsilon_{ki}=\frac{hc_0}{4\pi\lambda_{ki}}A_{ki}N_{\rm k}, \tag{5}$$

λ_{ki} is the wavelength of the emitted light. h is Planck constant. c_0 is the velocity of light in vacuum. A_{ki} is the transition probability (the probability that an atom in k state emits spontaneously in a random direction and gets de-excited to state i). Combining equations (5) and (3), we get

$$\frac{\varepsilon_{ki}\lambda_{ki}}{A_{ki}g_{\rm k}}=\frac{hc_0}{Z(T)}\exp\left|-\frac{E_{\rm k}}{KT_{\rm exc}}\right|. \tag{6}$$

Appling the logarithm to both sides of (6), we get

$$\ln\left(\frac{\varepsilon_{ki}\lambda_{ki}}{A_{ki}g_{\rm k}}\right)=-\frac{E_{\rm k}}{KT_{\rm exc}}+C, \tag{7}$$

in which C is a constant.

As stated above, according to the equation (7), we can fit a straight line with $E_{\rm k}$ in the horizontal axis and $\ln\left(\frac{\varepsilon_{ki}\lambda_{ki}}{A_{ki}g_{\rm k}}\right)$ in the vertical axis. And by finding the inverse of the slope of the fitting line, we can get the electron excitation temperature ($T_{\rm exc}$). In our study, the upper energy levels of the selected atomic transitions are assumed to be in LTE. Hence, the spectroscopic data used for measurement of the electron excitation temperature for the observed Ar-I emission lines are selected in Table 2. A Boltzmann plot of the chosen Ar-I lines is presented in Fig. 6.

Table 2　Parameters of Ar-I spectral lines for fitting electron excitation temperature[13].

λ/nm	$E_{\rm k}$/eV	$A_{ki}/(10^6{\rm s}^{-1})$	$g_{\rm k}$	Number of radiative transition
696.54	13.33	6.39	3	5
703.03	14.84	2.67	5	5
720.70	15.02	2.48	3	5
750.39	13.48	44.5	1	3
751.47	13.27	40.2	1	2
763.51	13.17	24.5	5	4

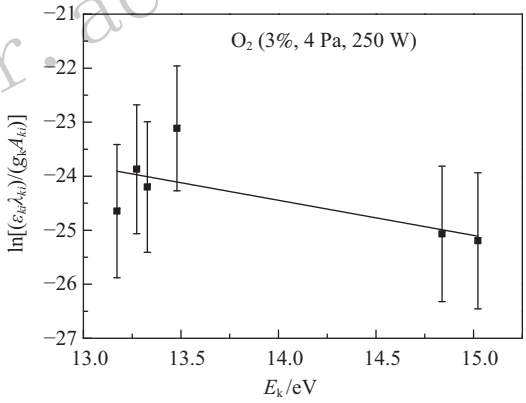

Fig. 6　(color online) Boltzmann plot obtained from Ar-I lines selected in table 2 at 3% O_2, pressure of 4 Pa and forward power of 250 W.

5　Results and discussion

5.1　Ar/Ar-O_2 discharge condition

For the experiment, we take Ar as discharge gas and O_2 as reaction gas. In plasma processing, Ar ion bombardments via inert gas RF discharge can be used to etch hydrocarbon contaminants, and chemical reactions via an appropriate amount of O_2 in discharge can be used to oxidize hydrocarbon contaminants and produce volatile oxides. Presumably, argon is prone to be ignited because of its lower ionization energy (15.76 eV) compared with neon (21.56 eV) and helium (24.59 eV). In the experiment, the coupling factor is adjusted to 1 and TM010 electromagnetic mode is excited to induce Ar/Ar-O_2 plasma discharge. Under such a circumstance, the lowest pressure for plasma discharge is found to be 2 Pa. With further experiment, we observe

the colors of plasma varying from red to grey with the change of the input RF power and gas pressure, as shown in Fig. 7.

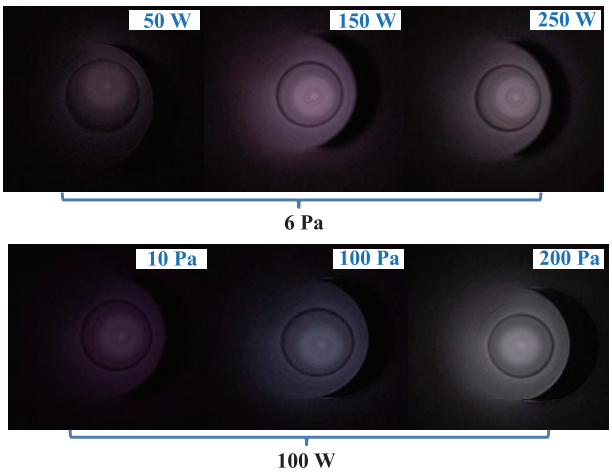

Fig. 7 (color online) The discharge drawings with different forward power and pressure in pure Ar.

To study the Ar/Ar-O_2 discharge condition, we explore the forward power of breakdown point and the power reflection coefficient in diverse pressure and oxygen content. In Fig. 8 and Fig. 9, the variation in forward power and power reflection coefficient of breakdown point for different pressure with pure argon is shown. It can be seen in Fig. 8 that the forward power of breakdown point decreases from 350 to 21 W as the pressure increases from 3 to 45 Pa. In the meantime, the power reflection coefficient tends to be a constant value with about 0.35. On the contrary, the forward power of breakdown point increases from 16 to 366 W and the power reflection coefficient decreases from 0.345 to 0.23 when the pressure increases from 50 to 650 Pa. We discover that the breakdown point decreases in the relative low pressure range (3∼45 Pa) and increases in the relative high pressure range (50∼650 Pa) with the gradual increase of pressure. Such results can be ascribed to the mean free path of electron (λ_e), which can be written as[14]

$$\lambda_e = \frac{3}{16\pi r^2 n_0}, \tag{8}$$

where r is the effective molecular radius, λ_e is the mean free path of electron, and n_0 is the initial total particle number density. On one hand, λ_e increases with the pressure going down. In the relative low pressure range, thus there will be less collisions, which is the major factor that's responsible for breakdown energy rising up with the decrease of the pressure. On the other hand, λ_e decreases with the pressure going up. Consequently, in the relative high pressure range, electron can't be accelerated for an adequate distance, which becomes the major factor that leads to the increase of breakdown energy with the pressure going up. Therefore there is a minimum breakdown energy with a suitable pressure.

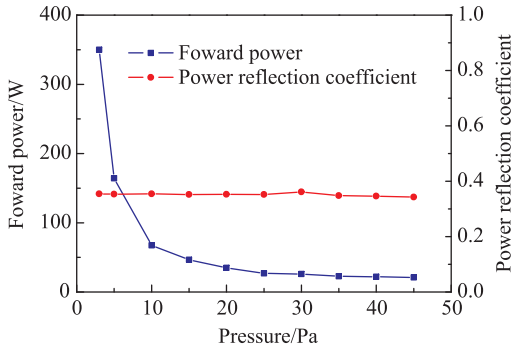

Fig. 8 (color online) Variation in forward power of breakdown point and power reflection coefficient for the low pressure of 3∼45 Pa with pure argon.

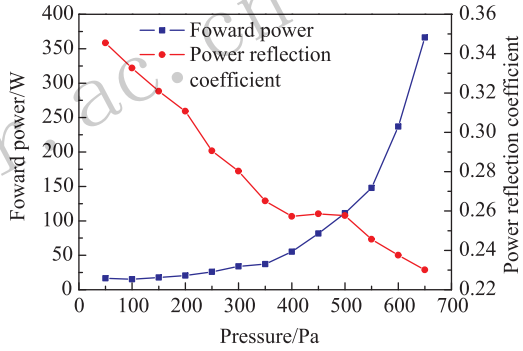

Fig. 9 (color online) Variation in forward power of breakdown point and power reflection coefficient for the low pressure of 50∼650 Pa with pure argon.

Fig. 10 and Fig. 11 show the forward power and power reflection coefficient of breakdown point for the low pressure of 2∼30 Pa in diverse O_2 content. It can be seen in Fig. 10 that the forward power of breakdown points are almost the same for the same pressure of

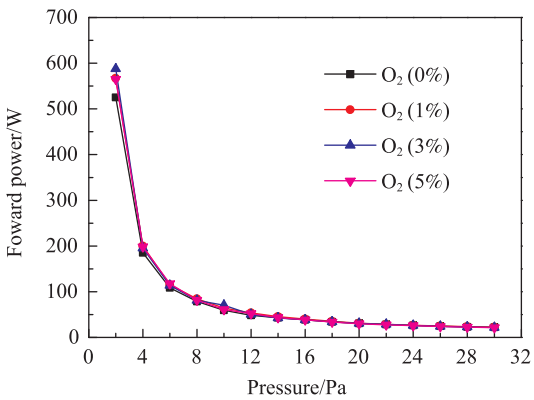

Fig. 10 (color online) The forward power of breakdown point for the low pressure of 2∼30 Pa in diverse O_2 content.

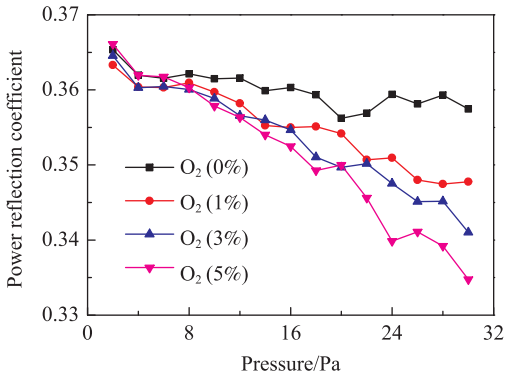

Fig. 11　(color online) The power reflection coefficient of breakdown point for the low pressure of 2∼30 Pa in diverse O_2 content.

different O_2 content. we can obtain from Fig. 11 that the power reflection coefficient of breakdown point decreases with the increase of pressure in the same O_2 content. In addition, the power reflection coefficient decreases with the increase of O_2 content in the same pressure.

5.2　Electron excitation temperature

Fig. 12 presents a typical optical emission spectrum from Ar(95%)/O_2(5%) plasma with a pressure of 2 Pa and a forward power of 150 W in the 1.3 GHz single-cell SRF cavity. Considering the the optical emission spectrum lines of interest, they can be categorized into three groups by the range of wavelength. The argon peaks are shown in 696.54, 703.03, 720.70, 750.39, 751.47 and 763.51 nm. The emission lines from Ar ion are presented at 450.99, 471.08 and 686.92 nm. In addition, The O peaks are shown in 615.67, 645.59 and 794.71 nm. In Ar/Ar-O_2 discharge, the emission intensity of 650∼900 nm is stronger than other wavelength range in optical emission spectrum.

In order to characterize the optical emission, electron excitation temperature is calculated with the use of Ar lines(Table 2) and conventional Boltzmann plot

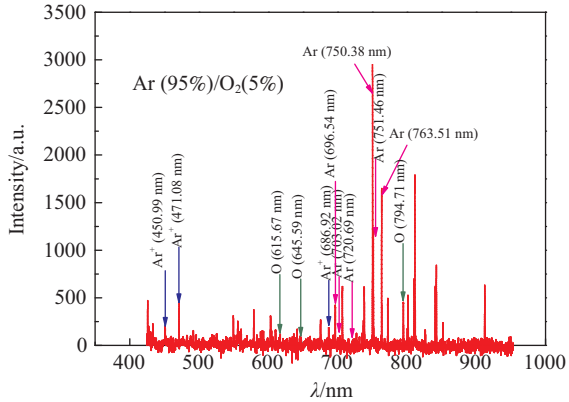

Fig. 12　(color online) A typical optical emission spectrum from Ar(95%)/O_2(5%) plasma at 2 Pa and 150 W in the 1.3 GHz single-cell SRF cavity.

method(Eq. (7)). The electron excitation temperature as functions of pressure and forward power are shown in Fig. 13(a) and Fig. 13(b). It should be emphasized that the plots present variation trend of the electron excitation temperature. Fig. 14 presents the variation of the electron excitation temperature with the variation of forward power and pressure in Ar(100%)/O_2(0%), Ar(99%)/O_2(1%), Ar(97%)/O_2(3%) and Ar(95%)/O_2(5%). It can be distinctly seen in Fig. 14 that the electron excitation temperature increases with decrease of pressure in identical forward power and O_2 content, while, the electron excitation temperature remains unchanged basically with increase of forward power in identical pressure and O_2 content. We can obtain from Eq. (8) that the mean free path of electron is inversely proportional to total particle number density. As a result, if the pressure is increased, then the mean free path of electron decreases, which results in a shorter distance for accelerating in the electric field and hence less average kinetic energy and lower electron excitation temperature[14]. The electron oscillation frequency, denoted by ω_p, is given by[15]

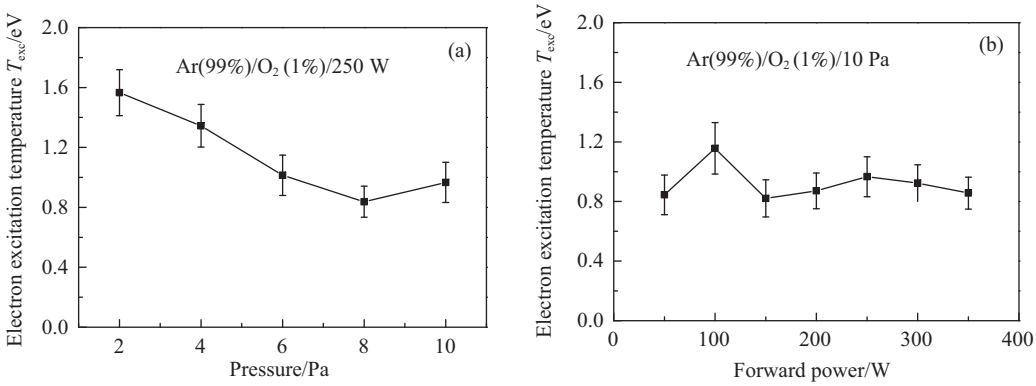

Fig. 13　Variation of the electron excitation temperature as a function of the pressure and forward power in Ar(99%)/O_2(1%)/250 W (a), Ar(99%)/O_2(1%)/10 Pa (b).

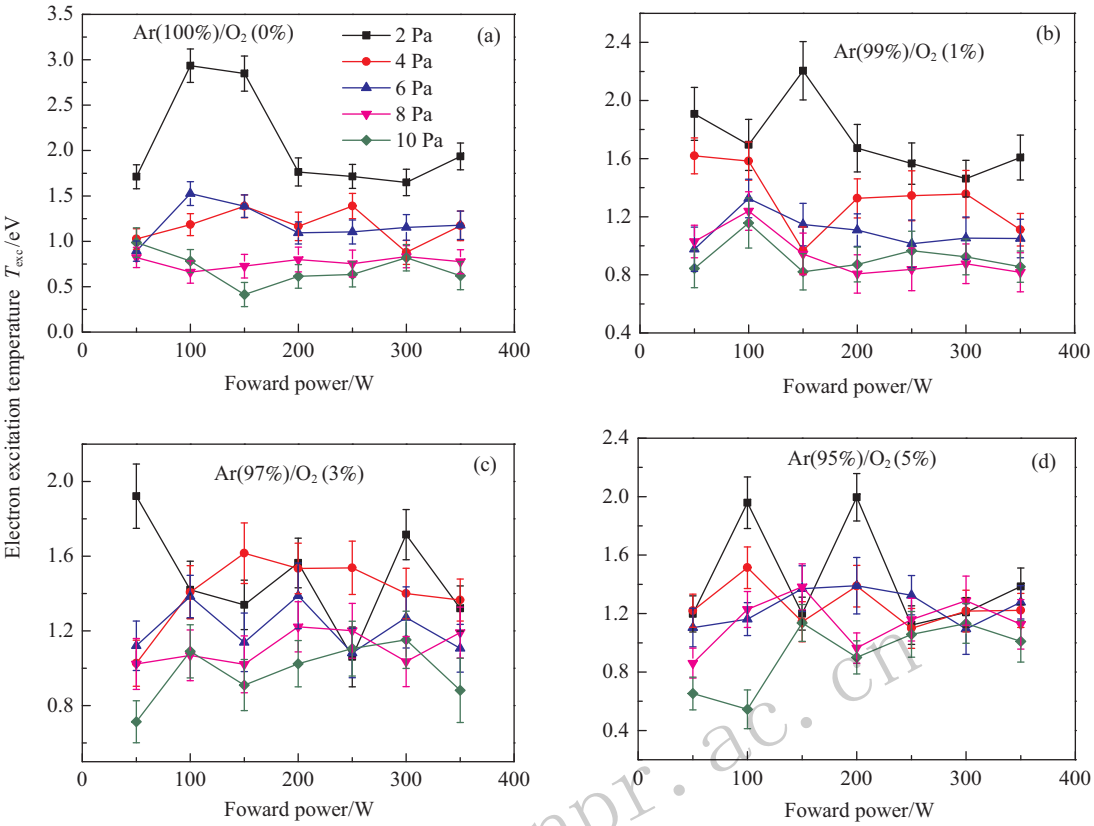

Fig. 14 (color online) Variation of the electron excitation temperature as functions of forward power and pressure in Ar(100%)/O_2(0%), Ar(99%)/O_2(1%), Ar(97%)/O_2(3%) and Ar(95%)/O_2(5%).

$$\omega_{\rm p}=\left(\frac{n_{\rm e}e^2}{m_{\rm e}\epsilon_0}\right)^{\frac{1}{2}}, \tag{9}$$

in frequency units, this gives approximately

$$f_{\rm p}=9\sqrt{n_{\rm e}(10^{12}{\rm cm}^{-3})}{\rm GHz}. \tag{10}$$

where $n_{\rm e}$ is the electron number density and the unit of $n_{\rm e}$ is 10^{12} cm^{-3} , $m_{\rm e}$ is the electron mass, e is electron charge and ϵ_0 is dielectric constant. $f_{\rm p}$ is called the plasma frequency (also called electron oscillation frequency or Langmuir frequency), and it depends only on the plasma density. A typical plasma density is 10^{10} cm^{-3}, thus, the plasma frequency is 0.9 GHz. On account of the low pressure and low temperature plasma in our research, it is assumed that the plasma density is less than 10^{10} cm^{-3} so that the plasma frequency is also less than 0.9 GHz. As a result, the plasma frequency in our experiments is less than the RF frequency (1.3 GHz). Hence, the electron excitation temperature has changed hardly with increase of forward power in identical pressure and O_2 content.

5.3 Residual gas analysis

Based on the above discussion, the Ar/O_2 plasma processing is carried out with the O_2(3% or 5%), forward power (50∼250 W) and pressure (2∼16 Pa) in the 1.3 GHz single-cell SRF cavity. In order to avoid excessive heat accumulation in the inner surface of the cavity, a pulse power is adopted in the Ar/O_2 plasma processing. A quadrupole mass spectrometer is used to analyze the residual gas during Ar/O_2 plasma discharge. In the Fig. 15, it can be seen that the CO peak and the downward O_2 peak are detected in the plasma processing and there are no the CO peak and the downward O_2 peak in the not discharge. Therefore,

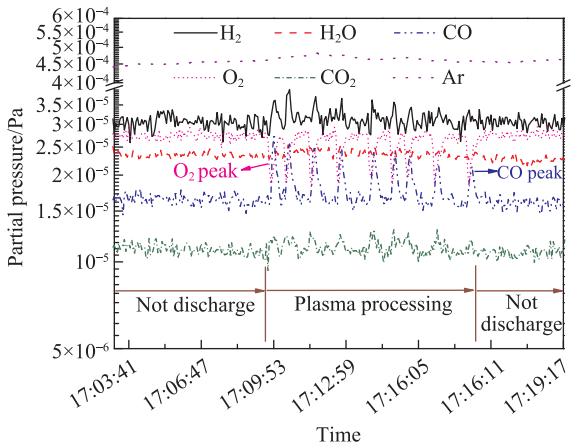

Fig. 15 (color online) Residual gas analysis of Ar/O_2 plasma processing in the 1.3 GHz single-cell SRF cavity.

in the plasma processing, O_2 is used to oxidize the carbide of the cavity inner surface so that CO is produced. It can be deduced that Ar/O_2 plasma processing can eliminate the carbide in the 1.3 GHz single-cell SRF cavity with the result of residual gas analysis.

6 Conclusions

In this paper, the plasma processing research experimental setup has been designed for a 1.3 GHz single-cell SRF cavity at room temperature. $Ar/Ar\text{-}O_2$ plasma is produced in the cavity with different forward power, gas pressure and O_2 content with the TM010 electromagnetic field mode and 1.0 coupling factor. It can be found that the forward power of breakdown point decreases from 350 to 21 W as the pressure increases from 3 to 45 Pa. In the meantime, the power reflection coefficient tends to be a constant value with about 0.35. On the contrary, the forward power of breakdown point increases from 16 W to 366 W and the power reflection coefficient decreases from 0.345 to 0.23 when the pressure increases from 50 to 650 Pa. In $Ar\text{-}O_2$ mixture discharge, the forward power of breakdown point can not be distinguished in the same pressure of different O_2 content. The power reflection coefficient of breakdown point decreases with the increase of pressure in the same O_2 content. In addition, the power reflection coefficient decreases with the increase of O_2 content in the same pressure. With the conventional Boltzmann plot method, the electron excitation temperature is evaluated and the change of the temperature is studied as functions of pressure, forward power and O_2 content. We discover that the electron excitation temperature increases with decrease of pressure in identical forward power and O_2 content, while, the electron excitation temperature remains unchanged basically with increase of forward power in identical pressure and O_2 content.

According to the result of residual gas analysis, O_2 is used to oxidize the carbide of the cavity inner surface so that CO is produced and it can be deduced that Ar/O_2 plasma processing can eliminate the carbide in the 1.3 GHz single-cell SRF cavity.

Acknowledgements This work is supported by the National Natural Science Foundation of China (Grant No. 91426303, 11475232 and 11535016).

References:

[1] PADAMSEE H, KNOBLOC J, HAYS T, *et al.* RF superconductivity for accelerators. New York: WILY-VCH, 2008.

[2] SCHWETTMAN A H, TURNEAURE P J, WAITES F R, *et al.* Journal of Applied Physics, 1974, **45**: 914.

[3] TYAGI V P, DOLEANS M, HANNAH B, *et al.* Appl Surf Sci, 2016, **369**: 29.

[4] DOLEANS M, TYAGI V P, AFANADOR R, *et al.* Nucl Instr Method A, 2016, **812**: 50.

[5] CST Simulation Packages, https://www.cst.com/.

[6] http://www.bbef-tech.com/.

[7] AHMED S, MAMMOSSER D J. Review of Scientific Instruments, 2015, **86**: 073303.

[8] GE M, FURUTA F, HOFFSTAETTER G, *et al.* Efforts of the Improvement of Cavity Q-Value by Plasma Cleaning Technology: Plan and Results from Cornell Unviversity[C]//Proceeding of SRF2015, 2015.

[9] LIEBERMAN M A, LICHTENBERG A J. Principle of Plasma Discharges and Materials Processing[M]. Hoboken: John Wiley & Sons, 2005.

[10] YOUNUS M, REHMAN U N, SHAFIQ M, *et al.* Physics of Plasmas, 2016, **23**: 083521.

[11] CHUNG H T, KANG R H, BAE K M, *et al.* Physics of Plasmas, 2012, **19**: 113502.

[12] GRIEM R H. Principles of Plasma Spectroscopy[M]. Cambridge: Cambridge University Press, 1997.

[13] https://www.nist.gov/pml/atomic-spectra-database/.

[14] WU H, ZHAO Y P, CUI H Y, *et al.* Diagnostics of Electron Temperature and Density in a Capillary Predischarge Ar Plasma[C]// International Academic Symposium on Optoelectronics and Microelectronics Technology, 2011.

[15] CHEN F F, CHANG J P. Lecture Notes on Principles of Plasma Processing. Los Angeles: Plenum/Kluwer Publishers, 2002.

1.3 GHz 单 cell 超导射频腔等离子体清洗放电研究

杨 磊[1,2]，吴安东[1,2]，卢 亮[1,†]，李永明[1]，徐显波[1]，陈 龙[1,2]，李晨星[1]，
孙列鹏[1]，李春龙[1]，马 伟[1,2]，何 涛[1,2]，邢超超[1,2]，何 源[1]

(1. 中国科学院近代物理研究所, 兰州 730000;
2. 中国科学院大学, 北京 100049)

摘要: 场致发射限制超导射频腔加速梯度增长。为了减少超导射频腔场致发射，在室温条件下，设计搭建了 1.3 GHz 单 cell 超导射频腔等离子体清洗实验装置，开展等离子体清洗放电研究。使用 CST 软件模拟腔中的电磁场分布并且优化外部品质因数得到合适的放电条件。随着压强、前向功率和含氧量的变化，实验探讨了 Ar/Ar-O_2 放电的物理特征和电子激发温度的变化趋势。残余气体分析结果表明，Ar/O_2 等离子体清洗能够消除腔体内表面的碳化物。

关键词: 等离子体清洗；Ar/Ar-O_2 放电条件；电子激发温度；超导射频技术

收稿日期: 2018-06-05； **修改日期:** 2018-07-22
基金项目: 国家自然科学基金资助项目(91426303, 11475232, 11535016)
† **通信作者:** 卢亮，E-mail: luliang@impcas.ac.cn。